

Jinyan Zhao^{1,2}, Liya Liu^{1,2}, Yuchen Zhang^{1,2}, Yun Wan^{1,2}, Zhenfeng Hong^{1,2*}

¹Academy of Integrative Medicine Biomedical Research Center, Fujian University of Traditional Chinese Medicine, 1 Qiuyang Road, Shangjie Minhou, Fuzhou 350122, Fujian, China., ²Fujian Key Laboratory of Integrative Medicine on Geriatrics, Fujian University of Traditional Chinese Medicine, 1 Qiuyang Road, Shangjie Minhou, Fuzhou 350122, Fujian, China.

*Corresponding Author Email: Zfhong1953@163.com

Abstract

Background: Xiao-Chai-Hu Tang (XCHT) is an extract of seven herbs with anticancer properties, but its mechanism of action is unknown. In this study, we evaluated XCHT-treated hepatocellular carcinoma (HCC) for anti-proliferative and pro-apoptotic effects.

Materials and Methods: Using a hepatic cancer xenograft model, we investigated the *in vivo* efficacy of XCHT against tumor growth by evaluating tumor volume and weight, as well as measuring apoptosis and cellular proliferation within the tumor. To study the effects of XCHT *in vitro*, we measured the cell viability of XCHT-treated Huh7 cells, as well as colony formation and apoptosis. To identify a potential mechanism of action, the gene and protein expression levels of Bax, Bcl-2, CDK4 and cyclin-D1 were measured in XCHT-treated Huh7 cells.

Results: We found that XCHT reduced tumor size and weight, as well as significantly decreased cell viability both *in vivo* and *in vitro*. XCHT suppressed the expression of the proliferation marker Ki-67 in HCC tissues and inhibited Huh7 colony formation. XCHT induced apoptosis in HCC tumor tissues and in Huh7 cells. Finally, XCHT altered the expression of Bax, Bcl-2, CDK4 and cyclin-D1, which halted cell proliferation and promoted apoptosis.

Conclusion: Our data suggest that XCHT enhances expression of pro-apoptotic pathways, resulting in potent anticancer activity.

Key Words: Xiao-Chai-Hu Tang; proliferation; apoptosis; hepatocellular carcinoma

Introduction

Hepatocellular carcinoma (HCC) is one of the top five cancers diagnosed worldwide [El-Serag and Rudolph, 2007; Jemal et al, 2011]. HCC is the third leading cause of cancer-related deaths, and China will contribute close to half of the estimated 600,000 individuals who will succumb to the disease annually [Jemal et al, 2011; Sherman, 2005]. Surgical resection is the preferred treatment following HCC diagnosis, since removing the tumor completely offers the best prognosis for long-term survival. This treatment is suitable for only 10-15% of patients with early-stage disease, since tumor resection may disrupt vital functions or structures if the tumor is large or has infiltrated into major blood vessels [Levin et al, 1995]. For patients with advanced stage HCC, chemotherapy is the best therapeutic option available. Standard chemotherapeutic regimens can involve single agents or a combination of drugs such as doxorubicin, cisplatin or fluorouracil. Late stage HCC develops drug resistance to standard chemotherapeutic combinations, and less than 20% of patients with advanced liver cancer will respond to these treatment regimens [Abou-Alfa et al, 2008]. Identification of more effective anticancer therapies is needed to provide alternatives to standard chemotherapeutic regimens, as well as treatments for drug resistant HCC.

Complementary and alternative medicines (CAM) have received considerable attention in Western countries for their potential therapeutic applications [Xu et al, 2006; Cui et al, 2010]. Traditional Chinese medicine (TCM) has been used in the treatment of cancer for thousands of years in China and other Asian countries. These medicines have gained acceptance as alternative cancer treatments in the United States and Europe [Wong et al, 2001; Gai et al, 2008]. When TCM is combined with conventional chemotherapy, there is an increase in the sensitivity of tumors to chemotherapeutic drugs, a reduction in both the side effects and complications associated with chemotherapy or radiotherapy, and an improvement in patient quality of life and survival [Konkimalla and Efferth, 2008].

Xiao-Chai-Hu-Tang (XCHT) is an extract of seven herbs: Bupleurum chinense (Chai-Hu), Pinellia ternata (Ban-Xia), Scutellaria baicalensis (Huang-Qin or Chinese skullcap root), Zizyphus jujube var. inermis (Da-Zao or jujube fruit), Panax ginseng (Ren-Shen or ginseng root), Glycyrrhiza uralensis (Gan-Cao or licorice root), and Zingiber officinale (Sheng-Jiang or ginger rhizome). The formulation for XCHT was first recorded in Shang Han Za Bing Lun during the Han Dynasty, and the ancient methodology for preparing XCHT has been performed in China for thousands of years. In TCM, XCHT has traditionally been used to treat a variety of Shaoyang diseases (including disorders of

the liver and gallbladder). Common side-effects experienced with XCHT treatment include alternating chills and fever, but the medication is well-tolerated by the majority of patients. The relatively low toxicity of XCHT is an important characteristic for potential use of this extract in combinatorial therapies. Ancient scholars believed the mechanism of action of XCHT involved harmonizing the Shaoyang, where pathogens were eliminated through enhanced liver function and improved digestion. More recently, XCHT has been reported to be effective as an anti-cancer agent, although the precise mechanism of its tumoricidal activity remains unclear [Zhu et al, 2005; Shiota et al, 2002; Watanabe et al, 2001; Yano et al, 1994; Kato et al, 1998; Liu et al, 1998; Mizushima et al, 1995]. To gain further insights into the mechanism of action of this ancient extract, we examined the anti-proliferative and pro-apoptotic activities of XCHT on HCC.

Materials and Methods

Materials and Reagents

Dulbecco's Modified Eagle Medium (DMEM), fetal bovine serum (FBS), penicillin–streptomycin, trypsin-EDTA and TriZol reagents were purchased from Life Technologies (Carlsbad, CA, USA). PrimeScript™ RT reagent Kit with gDNA Eraser was purchased from Takara BIO Inc. (Tokyo, Japan). TUNEL assay kit was purchased from R&D Systems (Minneapolis, MN, USA). BCA Protein Assay Kit was purchased from Tiangen Biotech Co., Ltd. (Beijing, China). Antibodies for Bax, Bcl-2, CDK4 and CyclinD1 were obtained from Santa Cruz Biotechnology, Inc. (Santa Cruz, CA). All other chemicals, unless otherwise stated, were obtained from Sigma-Aldrich (St. Louis, MO, USA).

Preparation of Xiao-Chai-Hu-Tang (XCHT).

The Xiao-Chai-Hu-Tang extract was prepared by boiling 7 authenticated herbs in distilled water: 24.0g *Bupleurum chinense* root (Chai-Hu), 9.0g *Pinellia ternata* tuber (Ban-Xia), 9.0g *Scutellaria baicalensis* root (Huang-Qin), 9g *Zizyphus jujube var. inermis* fruit (Da-Zao or jujube fruit), 6g *Panax ginseng* root (Ren-Shen or ginseng), 5.0g *Glycyrrhiza uralensis* root (Gan-Cao or licorice), and 9.0g *Zingiber officinale* rhizome (Sheng-Jiang or ginger). The aqueous extraction was filtered and spray-dried. A stock solution of XCHT was prepared immediately prior to use by dissolving the XCHT powder in DMEM at a concentration of 250 mg/ml. The working concentrations of XCHT were obtained by diluting the stock solution in the culture medium.

Cell Culture

A human hepatoma cell line (Huh7) was purchased from Xiangya Cell Center (Hunan, China). Huh7 cells were grown in DMEM supplemented with 10% (v/v) FBS, 100 units/ml penicillin, and 100 µg/ml streptomycin. Huh7 cells were cultured at 37°C, in a 5% CO₂ humidified environment. The cells were subcultured at 80-90% confluency.

Animals

Male BALB /C athymic nude mice (with an initial body weight of 20–22 g) were obtained from SLAC Animal Inc. (Shanghai, China). Animals were housed in standard plastic cages under automatic 12 h light/dark cycles at 23 °C, with free access to food and water. All animals were kept under specific pathogen-free conditions. The animal studies were approved by the Fujian Institute of Traditional Chinese Medicine Animal Ethics Committee (Fuzhou, Fujian, China). The experimental procedures were carried out in accordance with the Guidelines for Animal Experimentation of Fujian University of Traditional Chinese Medicine (Fuzhou, Fujian, China).

In Vivo Xenograft Study

Hepatocarcinoma xenograft mice were produced using Huh7 cells. The cells were grown in culture, detached by trypsinization, washed, and resuspended in serum-free DMEM. Resuspended cells (4×10^6) mixed with Matrigel (1:1) were subcutaneously injected into the right flank of nude mice to initiate tumor growth. When tumor sizes reached 3 millimeters in diameter, mice were randomly divided into two groups (n =10) and treated with XCHT (dissolved in saline) or saline daily by intraperitoneal injection. All treatments were given 5 days a week for 21 days. Body weight and tumor size were measured. Tumor size was determined by measuring the major (L) and minor (W) diameters with a caliper. The tumor volume was calculated according to the following formula: tumor volume = $\pi/6 \times L \times W^2$. At the end of the experiment, the mice were anaesthetized with ether and sacrificed by cervical vertebra dislocation. The tumors were then excised and weighed. and tumor segments were fixed in buffered formalin and stored at -80°C for molecular analysis.

Assessment of Cell Viability by the MTT Assay.

Cell viability was assessed by the MTT colorimetric assay. Huh7 cells were seeded into 96-well plates at a

[doi:10.21010/ajtcam.v14i3.25](https://doi.org/10.21010/ajtcam.v14i3.25)

density of 1×10^4 cells/well in 0.1 ml medium. The cells were treated with various concentrations (0, 0.5, 1.0, 1.5 mg/ml) of XCHT for 24 h, 48 h and 72 h. At the end of the treatment, 100 μ l of MTT (0.5 mg/ml in PBS) were added to each well, and the samples were incubated for an additional 4 h at 37°C. The purple-blue MTT formazan precipitate was dissolved in 100 μ l DMSO. The absorbance was measured at 570 nm using an ELISA reader (BioTek, Model ELX800, USA).

Cell Morphology

Huh7 cells were seeded into 6-well plates at a density of 2×10^5 cells/ml in 2 ml DMEM. The cells were treated with 0, 0.5, 1.0, and 1.5 mg/mL of XCHT for 24 h. Cell morphology was observed using a phase-contrast microscope (Olympus, Japan), and the photographs were taken at a magnification of 200 \times .

Detection of Apoptosis with Hoechst Staining.

Huh7 cells were seeded into 12-well plates at a density of 1×10^5 cells/ml in 1 ml medium. After the cells were treated with XCHT for 24 h, apoptosis was visualized using the Hoechst staining kit as described in the manufacturer's instructions. Briefly, at the end of the treatment, cells were fixed with 4% polyoxymethylene and then incubated in Hoechst solution for 5–10 min in the dark. Images were captured using a phase-contrast fluorescence microscope (Leica, Germany) at a magnification of 400 \times .

Colony Formation

Huh7 cells were seeded into 6-well plates at a density of 2×10^5 cells/ml in 2 ml medium. After treatment with various concentrations (0, 0.5, 1.0, 1.5 mg/ml) of XCHT for 24 h, the cells were collected and diluted in fresh medium in the absence of XCHT and then reseeded into 6-well plates at a density of 1×10^3 cells/well. Following incubation for 8 days in a 37°C humidified incubator with 5% CO₂, the colonies were fixed with 10% formaldehyde, stained with 0.01% crystal violet and counted. Cell survival was calculated by comparing the survival of compound-treated cells to the control cells (normalized to 100% survival).

Apoptosis Detection in Hepatocarcinoma Tissues by TUNEL Staining.

Six tumors were randomly selected from XCHT-treatment or control groups. Tumor tissues were fixed in 10% formaldehyde for 48 h, paraffin-embedded and then sectioned into 4- μ m-thick slides. Samples were analyzed by TUNEL staining. Apoptotic cells were counted as DAB-positive cells (brown staining) in five arbitrarily selected microscopic fields at a magnification of 400 \times . TUNEL-positive cells were counted as a percentage of the total cells.

Immunohistochemistry Analysis of Hepatocarcinoma Tissues

Immunohistochemical staining for Ki-67 was performed as previously described. The sections were deparaffinized in xylene and hydrated through graded alcohols. Antigen retrieval was performed using heat treatment (placed in a microwave oven at 750 Watts for 7 minutes), in 10 mM sodium citrate buffer, pH 6.0. Sections were allowed to cool in the buffer at room temperature for 30 minutes, and the sections were then rinsed in deionised water three times for two minutes each. The endogenous peroxidase activity was blocked with 3% (v/v) hydrogen peroxide for 10 minutes. The sections were incubated with 1% bovine serum albumin in order to decrease non-specific staining and reduce endogenous peroxidase activity. The sections were then incubated with Ki-67 antibody (1:100 dilution), at 4° C over night using a staining chamber. After rinsing three times in PBS, sections were incubated in biotinylated goat anti-rabbit IgG (Boshide Wuhan, China), followed by treatment with an avidin–biotin–peroxidase complex (Vector). Immunostaining was visualized by incubation in 3,3-diaminobenzidine (DAB) as a chromogen. Sections were counterstained with haematoxylin. The Ki-67 positive immunostaining was visualized using a Nikon Eclipse 50i microscope (40 \times objective). The evaluation of Ki-67 expression was analyzed in 5 different fields, and the mean percentage of Ki-67 positive staining was evaluated. To rule out any non-specific staining, PBS was used in place of the primary antibody as a negative control.

RNA Extraction and RT-PCR Analysis

The expression of Bax, Bcl-2, CDK4 and CyclinD1 genes in HCC tissues or cells was analyzed by RT-PCR. Total RNA was isolated with TriZol Reagent according to the manufacturer's instructions. 1 μ g of total RNA was used to synthesize cDNA using the SuperScript II reverse transcriptase Kit (AMV) (TaKaRa, Tokyo, Japan). The reaction contained RNA, selected primers, and 10 μ l of the RT-PCR master mix: 10 mM Tris–HCl (pH8.3), 50 mM KCl, 5 mM MgCl₂, 1 unit/ μ l RNase inhibitor, 0.25 unit/ μ l AMV reverse transcriptase, 2.5 ml random primer, and 1 mM each of dATP, dGTP, dCTP and dTTP. Reverse transcription was performed for 1 hour at 42°C. The obtained cDNA was used to determine the mRNA amount of Bax, Bcl-2, CDK4 and cyclin-D1 by PCR. GAPDH was used as an internal control.

Samples were analyzed by gel electrophoresis (1.5% agarose). The DNA bands were visualized using a gel documentation system (BioRad, Model Gel Doc 2000, USA).

The sequences of the primers used for amplification of CDK4, CyclinD1, Bcl-2, Bax and GAPDH transcripts are as follows: CDK4 forward, 5'-CAT GTA GAC CAG GAC CTA AGC-3' and reverse, 5'-AAC TGG CGC ATC AGA TCC TAG-3'; cyclin-D1 forward, 5'-TGG ATG CTG GAG GTC TGC GAG GAA -3' and reverse, 5'-GGC TTC GAT CTG CTC CTG GCA GGC -3'; Bcl-2 forward, 5'-CAG CTG CAC CT GAC GCC CTT-3 and reverse, 5'-GCC TCC GTT ATC CTG GAT CC-3'; Bax forward, 5'-TGC TTC AGG GTT TCA TCC AGG-3' and reverse, 5'-TGG CAA AGT AGA AAA GGG CGA-3'; GAPDH forward, 5'-GTC ATC CAT GAC AAC TTT GG-3' and reverse, 5'-GAG CTT GAC AAA GTG GTC GT-3'.

Western Blotting Analysis

Four tumors were randomly selected from XCHT-treatment or control groups. Tumors were homogenized in nondenaturing lysis buffer and centrifuged at $14,000 \times g$ for 15 min. Protein concentrations were determined by BCA protein assay. Huh7 cells (2.0×10^5 cells/ml) in 5ml medium were seeded into 25 cm² flasks and treated with the indicated concentrations of XCHT for 24 h. Treated cells were lysed in mammalian cell lysis buffer containing protease and phosphatase inhibitor cocktails, and centrifuged at $14,000 \times g$ for 15 min. Protein concentrations in cell lysate supernatants were determined by BCA protein assay. Equal amounts of protein from each tumor or cell lysate were resolved on 12% SDS-PAGE gels using 80 V for 2 h and transferred onto PVDF membranes. The membranes were blocked for 2 h with 5% nonfat milk and incubated with the desired primary antibody directed against Bax, Bcl-2, CDK4, Cyclin D1, or β -actin (all diluted 1:1000) overnight at 4°C. Appropriate HRP-conjugated secondary antibodies (anti-rabbit or anti-mouse; 1:2000) were incubated with the membrane for 1 h at room temperature, and the membranes were washed again in TBS-T followed by enhanced chemiluminescence detection.

Statistical Analysis

All data are shown as the mean of three measurements. The data were analyzed using the SPSS package for Windows (Version 11.5). Statistical analysis of the data was performed using the Student's t-test and ANOVA. Differences with $P < 0.05$ were considered statistically significant.

Results

XCHT inhibits hepatocellular carcinoma (HCC) growth *in vitro* and *in vivo*.

We evaluated the *in vitro* anti-cancer activity of XCHT on the human hepatocellular carcinoma cell line Huh7 using the MTT assay. As shown in Figure 1A, treatment with 0.5-1.5 mg/ml of XCHT for 24, 48, or 72 reduced the viability of Huh7 cells by 17.91-26.27%, 44.01-77%, and 64.8-86.71% ($P < 0.05$) compared to untreated controls. These results indicate that XCHT inhibits the growth of Huh7 cells in both dose- and time-dependent manners. To verify these results, we evaluated the effect of XCHT on Huh7 cell morphology using phase-contrast microscopy. As shown in Figure 1B, untreated Huh7 cells appeared as densely packed and disorganized multilayers. In contrast, many of the XCHT-treated cells were rounded, shrunken, and detached from adjacent cells, or floating in the medium. Taken together, these data demonstrate that XCHT inhibits the growth of Huh7 cells.

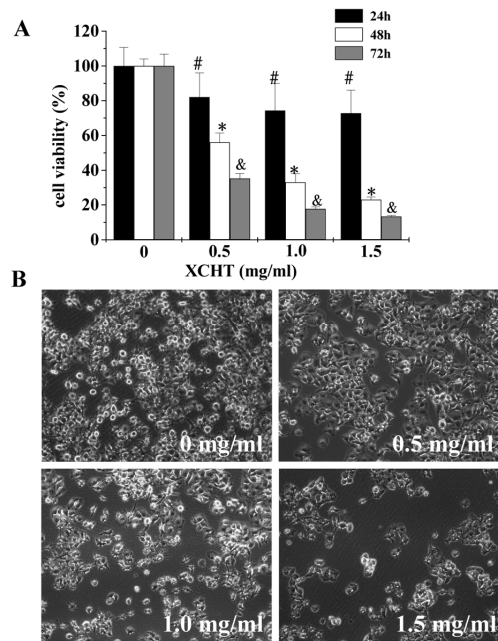


Figure 1: Effect of Xiao-Chai-Hu Tang (XCHT) on the viability and morphology of Huh7 cells. (A) Cell viability was determined by the MTT assay after Huh7 cells were treated with 0.5-1.5 mg/ml XCHT for 24, 48 or 72 h. The data were normalized to the viability of control cells (100%). Data are the averages with standard deviation (SD; error bars) from 3 independent experiments. The symbols (#), (*), and (&) indicate statistical significance compared to control cells ($P < 0.05$), for each indicated timepoint. (B) The Huh7 cells were treated with the 0.5-1.5 mg/ml XCHT for 24 h, and morphological changes were observed using phase-contrast microscopy. The images were captured at a magnification of 200 \times . Images are representative of 3 independent experiments.

To explore the anti-cancer activity of XCHT *in vivo*, we measured tumor volume and weight in HCC xenograft mice. As shown in Figure 2A and 2B, XCHT treatment significantly reduced both tumor volume and weight by Day 11 post-treatment. In contrast to tumors from the control group ($293.37 \pm 19.36 \text{ mm}^3$), XCHT treatment reduced tumor volume by 15.15% ($201.5 \pm 27.83 \text{ mm}^3$; $P < 0.05$). Tumor weight was reduced by 31.84% in XCHT-treated mice compared to control-treated mice ($P < 0.05$). Mice treated with XCHT demonstrated no changes in body weight during the course of the study, suggesting that XCHT treatment was relatively nontoxic to the animals (Figure 2C). Taken together, these data suggest that XCHT inhibits HCC growth both *in vivo* and *in vitro*, without apparent adverse effects.

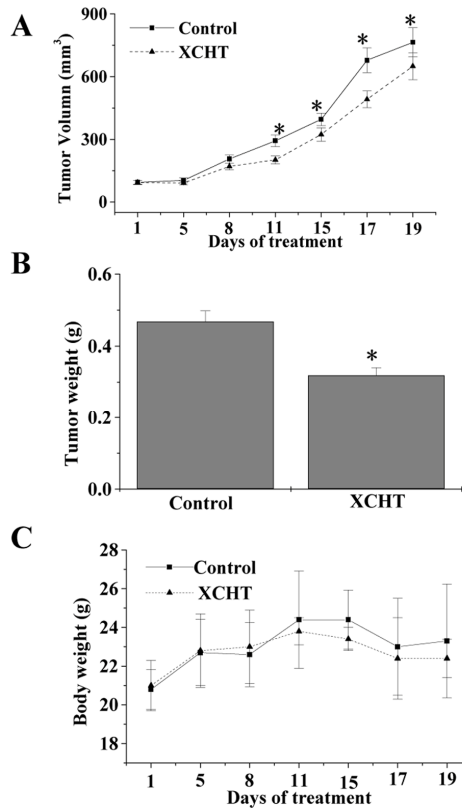


Figure 2: Effect of XCHT on tumor growth in hepatocellular carcinoma (HCC) xenograft mice. After tumor development, the mice were given intra-gastric administration of 14.2 g/kg of XCHT or PBS daily for 21 days. Tumor volume (A), tumor weight (B), and body weight (C) were measured. Data shown are averages with SD (error bars) from 10 mice in each group (n = 10). *P < 0.05, versus controls.

XCHT inhibits HCC proliferation *in vivo* and *in vitro*

One of the hallmarks of oncogenesis is unchecked cell proliferation, but the anti-proliferative activity of XCHT on hepatocarcinoma tumors was unknown. To measure the effect of XCHT on cell proliferation, we examined XCHT-treated tumors for a marker expressed by proliferating cell nuclei (Ki-67) using immunohistochemical staining (IHC). As shown in Figure 3A, the percentages of Ki-67 positive cells in tumor tissues from control and XCHT-treated xenograft mice were $76.0 \pm 9.6\%$ and $51 \pm 15.3\%$, respectively ($P < 0.05$). To examine the anti-proliferative activity of XCHT *in vitro*, Huh7 cells were treated with 0.5-1.5 mg/ml of extract and colony formation was measured. As shown in Figure 3B, treatment with increasing concentrations of XCHT for 24 h reduced the cell survival rate by 55.3%, 69.8% and 92.8% compared to untreated controls ($P < 0.05$). These results suggest that XCHT can inhibit HCC cell proliferation both *in vivo* and *in vitro*.

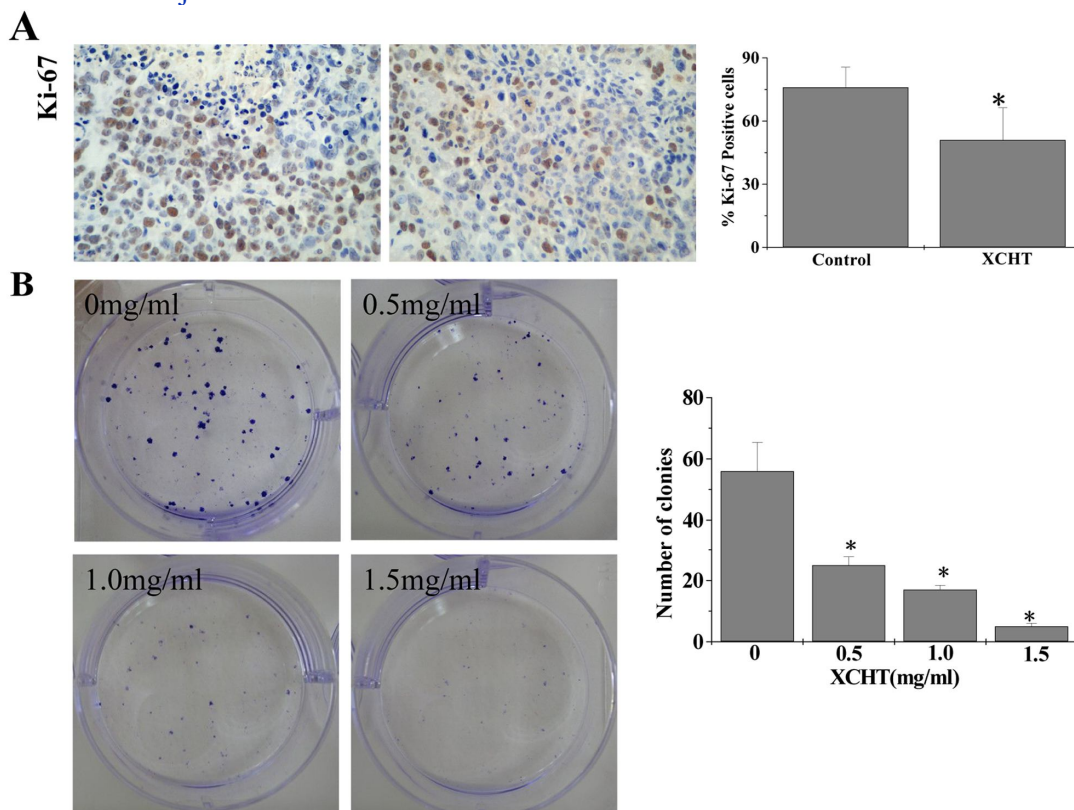


Figure 3: Effect of XCHT on cell proliferation in HCC xenograft mice and Huh7 cells. (A) Ki-67 assay in tumor tissues (400 ×). Data shown are averages with SD (error bars) from 6 individual mice in each group (n = 6). * $P < 0.05$, versus controls. (B) Huh7 cell colony formation assay. Data are averages with SD (error bars) from at least three independent experiments. * $P < 0.01$, versus control cells.

XCHT induces apoptosis of hepatocellular carcinoma cells *in vivo* and *in vitro*.

Apoptosis within HCC tumor tissues was visualized by IHC staining using the TUNEL assay. As shown in Fig 4A, XCHT-treated mice had a significantly higher percentage of TUNEL-positive cells ($82 \pm 15.3\%$) compared to the untreated control mice ($47 \pm 9.6\%$), indicating the pro-apoptotic effect of XCHT *in vivo*. To visualize the pro-apoptotic activity in XCHT-treated Huh7 cells, we evaluated changes in nuclear morphology using the DNA-binding dye Hoechst 33258. As shown in Fig 4B, XCHT-treated cells revealed condensed chromatin and a fragmented nuclear morphology, and these characteristics demonstrated typical apoptotic morphological features. In contrast, untreated cell nuclei showed a less intense but homogenous staining pattern, indicative of proliferating cells.

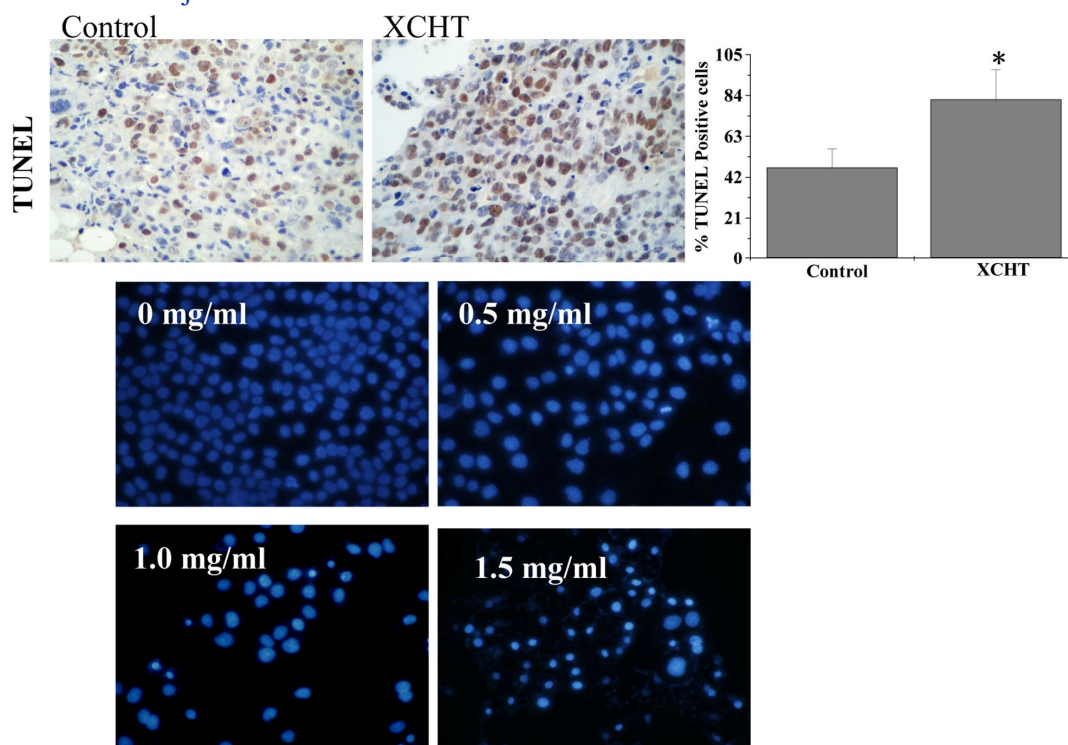


Figure 4: Effect of XCHT on apoptosis in both HCC xenograft mice and Huh7 cells. (A) TUNEL assay in tumor tissues (400 ×). Data shown are averages with SD (error bars) from 6 individual mice in each group (n = 6). * $P < 0.05$, versus controls; (B) Huh7 cells were treated with 0.5-1.5 mg/ml XCHT for 24 h and stained with Hoechst 33258. Images were visualized using a phase-contrast fluorescence microscope. The images were captured at a magnification of 400×. Images are representative of 3 independent experiments.

XCHT regulates the gene and protein expression correlated with apoptosis and proliferation *in vivo* and *in vitro*

Very little is known regarding the mechanism of action of XCHT, or the pathways that this extract targets to generate its anti-proliferative and pro-apoptotic activities. We examined the effect of XCHT treatment on the expression of correlated genes and proteins that are important regulators of apoptosis and proliferation using RT-PCR and western blotting. As shown in Fig 5A and B, XCHT significantly reduced both gene and protein expression of the anti-apoptotic factor Bcl-2 in HCC tumor tissues. In contrast, the gene and protein expression of the pro-apoptotic factor Bax increased after XCHT treatment. XCHT treatment significantly decreased the mRNA and protein expression levels of CDK4 and cyclin-D1 compared to the control group ($P < 0.05$). Correlating with our *in vivo* data from HCC tissues, Huh7 cells treated with XCHT demonstrated a significant reduction in the mRNA and protein expression levels of Bcl-2, CDK4 and cyclin-D1, and an increase in the expression of Bax *in vitro* (Fig 6A and B). Together these data suggest that XCHT promotes apoptosis and inhibits proliferation of HCC by increasing the pro-apoptotic Bax/Bcl-2 ratio and modulating the expression of cell cycle-regulatory genes.

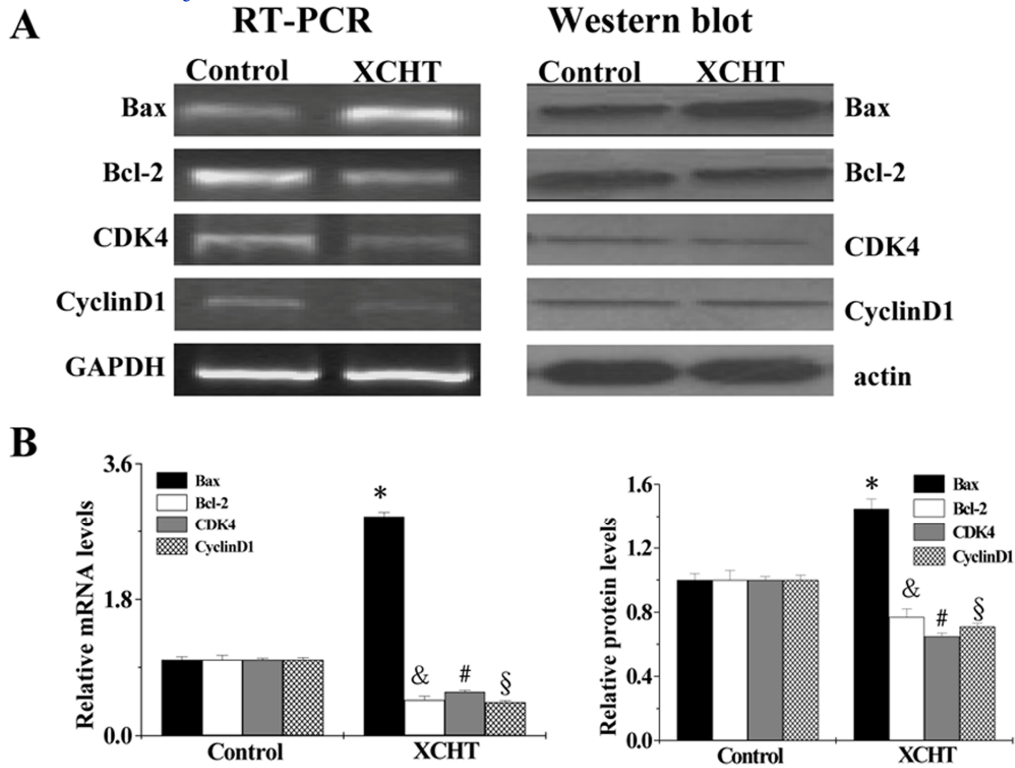


Figure 5: Effect of XCHT on the expression of Bcl-2, Bax, cyclin-D1 and CDK4 in HCC xenograft mice. (A) Four tumors were randomly selected from each group, and the mRNA or protein expression levels of Bcl-2, Bax, cyclin-D1, and CDK4 were determined by RT-PCR and Western blot analysis. GAPDH or β -actin were used as the internal controls. Data shown are representative samples. (B) Densitometric analysis of gene and protein expression levels. The data were normalized to the mean mRNA or protein expression levels of untreated control mice (100%). The symbols (*), (&), (#), and (§) indicate statistical significance versus controls ($P < 0.05$), for Bax, Bcl-2, CDK4 or cyclin-D1.

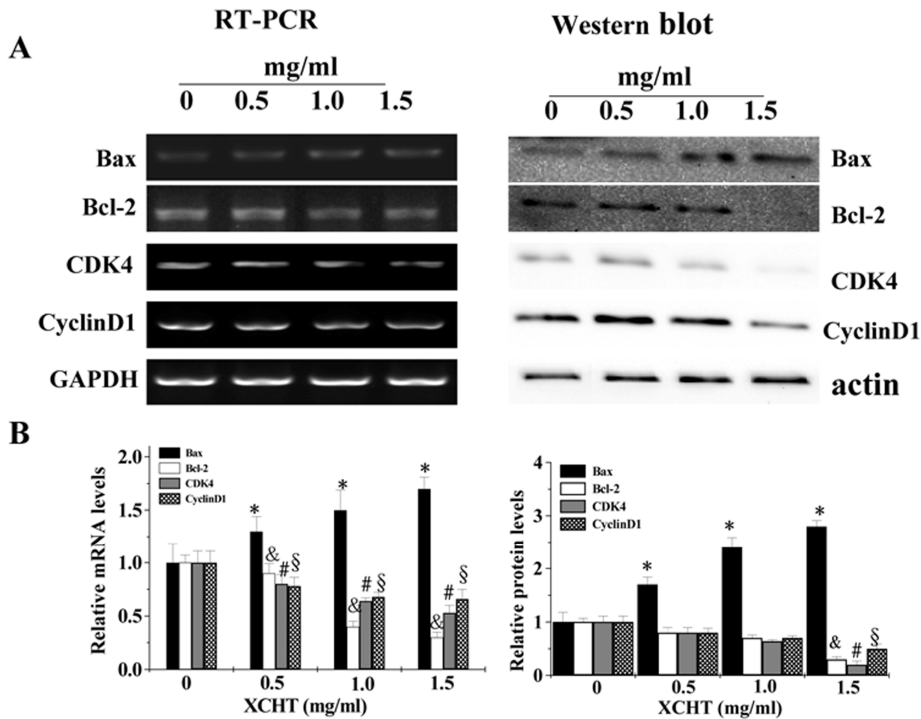


Figure 6: Effect of XCHT on the expression of Bcl-2, Bax, cyclin-D1 and CDK4 in Huh7 cells. The cells were treated with 0.5-1.5 mg/ml XCHT for 24 h. (A) The mRNA and protein levels of Bcl-2, Bax, CDK4 and cyclin-D1 were

determined using RT-PCR or western blotting. GAPDH or β -actin were used as the internal controls. The data are representative of three independent experiments. (B) Densitometric analysis of gene and protein expression levels. The data were normalized to the mean mRNA or protein expression of the untreated control cells (100%). The symbols (*), (&), (#), and (§) indicate statistical significance compared to control cells ($P < 0.05$), for Bax, Bcl-2, CDK4 or cyclin-D1.

Discussion

Xiao-Chai-Hu Tang (XCHT) is one of the most widely used Chinese herbal preparations, and it has long been used for the treatment of chronic liver diseases in China and other Asian countries. In the present study, we investigated its anti-tumor and anti-proliferative activities. Our findings suggest that XCHT could promote apoptosis and inhibit cellular proliferation in liver cancer.

Cancer cells are characterized by an uncontrolled increase in cell proliferation and/or a reduction in apoptosis [Adams and Cory, 2007]. Cell cycle deregulation is a hallmark of tumor cells, and targeting the proteins that mediate critical cell cycle processes is an emerging strategy for the treatment of cancer [Stewart et al, 2003]. The G1/S transition is one of the two main checkpoints of the cell cycle [Nurse, 1994], which is responsible for initiation and completion of DNA replication. G1/S progression is strongly regulated by cyclin-D1, which exerts its function by forming an active complex with its CDK major catalytic partners (CDK4/6) [Morgan, 1995]. An unchecked or hyperactivated cyclin-D1/CDK4 complex often leads to uncontrolled cell division and malignancy [Harakeh et al, 2008; Kessel and Luo, 2000; Chen et al, 1996; Zafonte et al, 2000]. Examination of cyclin-D1 and CDK4 expression levels during XCHT treatment demonstrated that XCHT suppresses the expression of both factors in HCC xenograft tissues and in Huh7 cells.

Apoptosis is important for embryogenesis, tissue homeostasis and defence against pathogens. Notably, apoptotic resistance is one of the main causes of tumorigenesis and tumor drug resistance [Cory and Adams, 2002; Lee and Schmitt, 2003]. The Bcl-2 family plays a critical role in apoptotic regulation. Pro-apoptotic Bax promotes intrinsic apoptosis by forming oligomers in the mitochondrial outer membrane, which facilitates the release of the apoptogenic molecules. In contrast, anti-apoptotic Bcl-2 blocks mitochondrial apoptosis by inhibiting the release and oligomerization of Bax [Leibowitz and Yu, 2010]. XCHT can induce apoptosis and overcome the apoptotic resistance of hepatocarcinoma cells *in vitro* and *in vivo*, which elevates the potential of this extract for development as an effective chemotherapy agent for treating HCC.

Conclusion

In conclusion, we demonstrate for the first time that XCHT can inhibit proliferation and induce apoptosis in liver cancer by regulating the expression of the Bcl-2 protein family and decreasing CDK4 and cyclin-D1 levels. Although the active ingredient and precise mechanism of action are not known, this research provides a starting point for exploring an XCHT-related HCC cancer therapy.

Acknowledgments

The project (No. 81303125) supported by National Natural Science Foundation of China. We thank Clarity Manuscript Consultants LLC for assistance with editing the manuscript.

Conflict of interest

The authors declare no financial or commercial conflicts of interest.

References

1. Abou-Alfa GK, Huitzil-Melendez FD, O'Reilly EM, Saltz LB. Current management of advanced hepatocellular carcinoma. *Gastrointest Cancer Res* (2008), 2 (2): 64-70.
2. Adams JM, Cory S. The Bcl-2 apoptotic switch in cancer development and therapy. *Oncogene* 2007, 26(9): 1324–1337.
3. Chen Y, Robles AI, Martinez LA, Liu F, Gimenez-Conti IB and Conti CJ. Expression of G1 cyclins, cyclin - dependent kinases, and cyclin- dependent kinase inhibitors in androgen- induced prostate proliferation in castrated rats. *Cell Growth Differ* 1996, 7(11): 1571 -1578.
4. Cory S, Adams JM. The Bcl2 family: regulators of the cellular life-or-death switch. *Nat Rev Cancer*. 2002, 2(9): 647–656
5. Cui X, Wang Y, Kokudo N, Fang D, Tang W. Traditional Chinese medicine and related active compounds against hepatitis B virus infection. *Biosci Trends*. 2010, 4 (2): 39-47.
6. El-Serag HB, Rudolph KL. Hepatocellular carcinoma: epidemiology and molecular carcinogenesis.

- Gastroenterology 2007, 132 (7): 2557-76.
7. Gai RY, Xu HL, Qu XJ, Wang FS, Lou HX, Han JX, Nakata M, Kokudo N, Sugawara Y, Kuroiwa C, Tang W. Dynamic of modernizing traditional Chinese medicine and the standards system for its development. *Drug Discov Ther* 2008, 2 (1): 2-4.
 8. Harakeh S, Abu-El-Ardat K, Diab-Assaf M, Niedzwiecki A, El-Sabban M, Rath M. Epigallocatechin-3-gallate induces apoptosis and cell cycle arrest in HTLV-1-positive and -negative leukemia cells. *Med. Oncol.* 2008, 25(1), 30–39.
 9. Jemal A, Bray F, Center MM, Ferlay J, Ward E;Forman D: Global cancer statistics. *CA Cancer J Clin* 2011, 61 (2): 69-90.
 10. Kato M, Liu W, Yi H, Asai N, Hayakawa A, Kozaki K, Takahashi M, Nakashima I. The herbal medicine Sho-saiko-to inhibits growth and metastasis of malignant melanoma primarily developed in ret-transgenic mice. *J Invest Dermatol* 1998, 111(4):640-644.
 11. Kessel D, Luo Y. Cells in cryptophycin-induced cell-cycle arrest are susceptible to apoptosis. *Cancer Lett.* 2000, 151(1), 25–29.
 12. Konkimalla VB, Efferth T. Evidence-based Chinese medicine for cancer therapy. *J Ethnopharmacol* 2008; 116 (2): 207-210.
 13. Lee S, Schmitt CA. Chemotherapy response and resistance. *Curr Opin Genet Dev*, 2003, 13(1): 90–96.
 14. Leibowitz B, Yu J. Mitochondrial signaling in cell death via the Bcl-2 family. *Cancer Biol Ther* 2010, 9 (6): 417–422.
 15. Levin B and Amos C. Therapy of unresectable hepatocellular carcinoma. *N Engl J Med* 1995, 332 (19): 1294–1296.
 16. Liu W, Kato M, Akhand AA, Hayakawa A, Takemura M, Yoshida S, Suzuki H, Nakashima I. The herbal medicine sho-saiko-to inhibits the growth of malignant melanoma cells by upregulating Fas-mediated apoptosis and arresting cell cycle through downregulation of cyclin dependent kinases. *Int J Oncol* 1998, 12(6):1321-1326.
 17. Mizushima Y, Kashii T, Tokimitsu Y, Kobayashi M. Cytotoxic effect of herbal medicine sho-saiko-to on human lung-cancer cell-lines in-vitro. *Oncol Rep* 1995, 2(1):91-94.
 18. Morgan DO. Principles of CDK regulation. *Nature* 1995, 374 (6518): 131–134.
 19. Nurse P. Ordering S phase and M phase in the cell cycle. *Cell* 1994, 79(4):547–550.
 20. Sherman M. Hepatocellular carcinoma: epidemiology, risk factors, and screening. *Semin Liver Dis* 2005, 25 (2): 143-154.
 21. Shiota G, Maeta Y, Mukoyama T, Yanagidani A, Udagawa A, Oyama K, Yashima K, Kishimoto Y, Nakai Y, Miura T, Ito H, Murawaki Y, Kawasaki H. Effects of Sho-Saiko-to on hepatocarcinogenesis and 8-hydroxy-2'-deoxyguanosine formation. *Hepatology* 2002, 35(5):1125-1133.
 22. Stewart ZA, Westfall MD, Pietenpol JA. Cell-cycle dysregulation and anticancer therapy. *Trends Pharmacol Sci* 2003, 24(3): 139–145.
 23. Watanabe S, Kitade Y, Masaki T, Nishioka M, Satoh K, Nishino H. Effects of lycopene and Sho-saiko-to on hepatocarcinogenesis in a rat model of spontaneous liver cancer. *Nutr Cancer* 2001;39(1):96-101.
 24. Wong R, Sagar CM, Sagar SM. Integration of Chinese medicine into supportive cancer care: A modern role for an ancient tradition. *Cancer Treat Rev* 2001, 27 (4): 235-246.
 25. Xu W, Towers AD, Li P, Collet JP. Traditional Chinese medicine in cancer care: Perspectives and experiences of patients and professionals in China. *Eur J Cancer Care (Engl)* 2006,15 (4): 397-403.
 26. Yano H, Mizoguchi A, Fukuda K, Haramaki M, Ogasawara S, Momosaki S, Kojiro M. The herbal medicine sho-saiko-to inhibits proliferation of cancer cell lines by inducing apoptosis and arrest at the G0/G1 phase. *Cancer Res* 1994 Jan 15;54(2):448-454.
 27. Zafonte BT, Hulit J, Amanatullah DF, Albanese C, Wang C, Rosen E, Reutens A, Sparano JA, Lisanti MP, Pestell RG. Cell-cycle dysregulation in breast cancer: Breast cancer therapies targeting the cell cycle. *Front Biosci* 2000, 5, D938–D961.
 28. Zhu K, Fukasawa I, Furuno M, Inaba F, Yamazaki T, Kamemori T, Kousaka N, Ota Y, Hayashi M, Maehama T, Inaba N. Inhibitory effects of herbal drugs on the growth of human ovarian cancer cell lines through the induction of apoptosis. *Gynecol Oncol* 2005, 97(2):405-409.